Active reduction of audible noise exciting radial force-density waves in induction motors

D. Franck, M. van der Giet, K. Hameyer

***Abstract*—This paper presents an approach to the active reduction of radial force-density waves. Additional flux-density waves are generated by the injection of additional and particular low-power current harmonics. With these flux-density waves a force-density countershaft to an acoustic annoying radial force density wave is generated. In this contribution a mathematical model to estimate the amplitude, frequency and phase shift of the required current harmonic is presented. The prediction of the phase-shift is strongly dependent on saturation effects and on the interaction of the additionally imposed and existing flux-density waves. Therefore, a finite element (FE) experiment set is proposed to increase the accuracy of the analytically predicted phase angle. The active injection of force-density countershafts is performed, analyzed and evaluated. The assessment is performed based on FE simulations. The authors found that the injection of force-density countershafts is applicable for force-density waves with any circumferential oscillation modes and frequency in general. However, the consideration of oscillation modes is limited to $r = 0$, $\pm 2p$, $\pm 3p$ and $\pm 4p$ in order to keep the additional losses in the machine within an acceptable limit. The proposed approach is robust concerning the accuracy of the phase shift of the additionally imposed current harmonic.**

***Index Terms*—Acoustic optimization, audible noise, noise and vibration, induction machine**

List of symbols

I	phase current
ξ	ordinal number of stator current frequency
ω	angular frequency
t	time
x	circumferencial coordinate, rad
k	phase number
B	flux-density
p	number of pole pairs
m	number of phases
q	number of slots per pole and phase
μ_0	permeability of free space
N	number of turn of the stator coil
δ	air-gap length
ν	number of pole pairs of field harmonics
k_w	winding factor
Λ	permeance function of stator and rotor
λ_1	stator permeance function
λ_2	rotor permeance function
φ	phase angle
g, k, l	integer
σ	force-density
m_i	expansion of fundamental frequency
Θ	magnetomotive-force
A	band-factor
f	frequency
r	force density mode order

Subscripts

ξ	frequency order
1	stator
2	rotor
k,l	wave number
$+$	denotes additional
counter	denotes countershaft
fund	denotes fundamental
b+	additional flux-density wave
i+	additional current harmonic

All authors are with the Institute of Electrical Machines - RWTH Aachen University, Germany phone: +49 241 80 97667, e-mail: david.franck@iem.rwth-aachen.de

I. Introduction

The acoustic radiation of electrical drives is attracting particular attention. On the one hand *PWM* supply of variable speed drives and on the other hand increasing torque-densities yield higher harmonic content of the magnetic air-gap field and ultimately this leads to higher audible noise excitations. There are various approaches to realize a low audible noise design of electrical machines. One can distinguish two major approaches to reduce the electromagnetic sources of the audible noise. The first one is the design of the machine, considering the combination of stator- and rotor-slots for induction motors, the winding-scheme, air-gap length, skew of the rotor-bars, the teeth geometry, etc. This parameters have a significant influence on the air-gap field harmonics. The fundamentals of estimating and reducing the audible noise by means of these parameters is strongly dependent on the application. The basic approach for an estimation and reduction of audible noise in this way are for example given in the literature [1], [2].

Addressing the power electronics supply of an electrical machine is a second way to influence the acoustic radiation. In the literature different approaches are presented. For example [3]–[7] propose a variation of the *PWM* frequency, which leads to a spreading of the tonal noise to atonal noise and a reduction of the harmonic content in the supply voltage. [8] proposes an alternative *PWM* strategy considering the A-weighted sound power level that takes into account the influence of the human ear on the prediction. The papers [9]–[11] propose to inject current harmonics in order to generate force-density countershafts. This approach is based on the rotating field theory and a detailed knowledge of the machine and its air-gap field harmonics is essential. However, the authors follow an experimental approach to determine the amplitude and the phase shift of the injected current harmonic. Only the frequency of the additional current is calculated in advance.

In this paper, an analytic description based on the rotating field theory [1], [6], [12], [13] is proposed to completely describe the effect of additionally imposed current harmonics in frequency, amplitude and phase on the air-gap field and the force density excitation. A similar approach has for example been proposed in [14], [15] for harmonic torque suppression. The approach is applied to a standard induction motor and validated by means of a finite element (FE) simulation.

II. Rotating field theory

The objective of the presented research is the reduction of particular force-density waves by means of injecting countershaft, i.e. a force-density wave, which has the same amplitude, frequency and circumferential mode compared to the annoying force-density wave, but is 180 degree phase shifted. The idea is based on the classical rotating field theory. A current in the stator winding of a poly-phase electrical machine generates flux-density waves, leading to radial force-density waves. These force-density waves can result in unacceptable acoustic noise radiation. A summary of the required equations for the squirrel cage induction motor are for example given in [12]. A short outline of the rotating field is given based on this paper here. Basis for the field generation of polyphase electrical machines is the phase current. The presented approach to calculate the air-gap field is based upon the assumption of ideal soft-magnetic material properties. This results in a linear-time-invariant equation system, which allows for the separation of the different field effects, such as the permeance variation due to slotting, winding distribution space harmonics and current time harmonics. Each effect is modeled individually and a linear superposition is applied to calculate the resulting air-gap field. For this purpose, the phase current is defined as

$$I = \sum_{\xi} \hat{I}_{\xi} \cdot \cos\left(\xi\left(\omega \cdot t - \frac{k-1}{3} \cdot 2\pi\right)\right) \tag{1}$$

whereby ξ denotes the ordinal number of the stator current frequency, ω the fundamental angular frequency of the stator current and k the phase number (i.e. $1, 2, 3$). The air-gap field can then be calculated according to [12]

$$\begin{aligned} B(x,t) = &\sum_{\xi}\sum_{\nu} 2p \cdot m \cdot q \cdot \frac{\mu_0 N}{2\pi\delta\nu} \cdot k_{\omega} \cdot \Lambda \cdot I \cdot \\ &\cos\left(\xi(\omega t - \nu x - \varphi)\right); \\ &\nu = p\left(6g + \xi\right); g \in Z; \xi \in N \end{aligned} \tag{2}$$

The permeance function of stator λ_1 and rotor λ_2 can be calculated individually by means of conformal mapping [16] and the resulting permeance function can be approximated by $\Lambda = \lambda_1 \cdot \lambda_2$. The formalism is for example presented in [17] or [12]. The current in the rotorbars can be calculated from the sator field [12]. This paper utilizes the fundamental field harmonic of the stator for the generation of the countershaft. Therefore, the rotor field is not described in more detail. All parasitic effects introduced by the additional current harmonics are evaluated based on FEM simulations. The radial force-density distribution can be calculated by means of the Maxwell stress tensor. The force-density can be calculated by a convolution [18] of two flux-density waves B_l and B_k in frequency domain. The Maxwell stress tensor can be evaluated locally since ideal material properties are assumed. The radial force-density writes

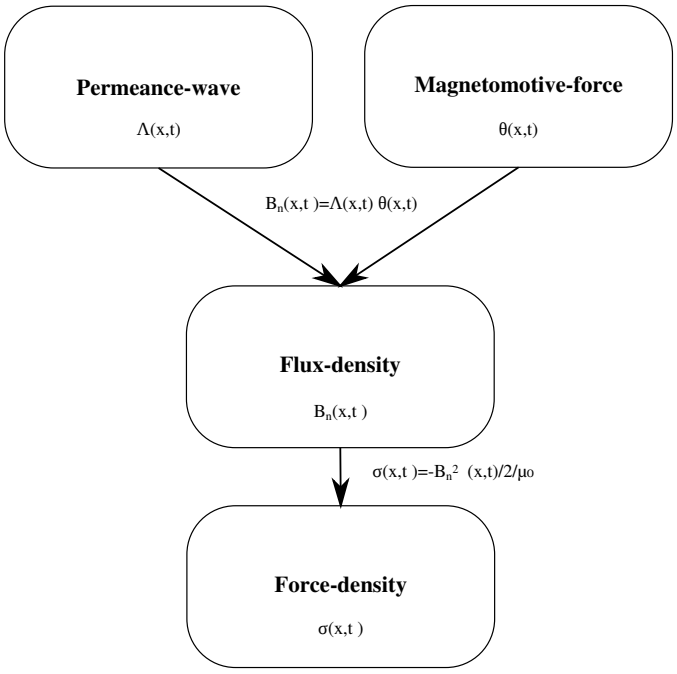

Figure 1. Generation of force-density waves.

$$\begin{aligned} \sigma(x,t) = -\sum_{k}\sum_{l} &\frac{1}{2\mu_0}\hat{B}_k\hat{B}_l \\ &\cos[(\nu_l \pm \nu_k)x - (\omega_l \pm \omega_k)t - (\varphi_l \pm \varphi_k)] \end{aligned} \tag{3}$$

A single radial force-density wave is, hence, created by a combination of two flux-density waves. The circumferential mode order, the frequency and the phase shift of the force-density wave can be calculated by the summation and subtraction of the ordinal numbers of the exciting flux-density waves. The presented theory is based on a Fourier-series-expansion of the air-gap field. The formalism to calculate the force-density waves is presented in Fig. 1.

The fundamental frequency for the series-expansion is the fundamental frequency of the stator current. Objective of the presented research is the systematic reduction of particular force-density waves by means of countershafts. In order to keep parasitic effects as small as possible, the countershaft is to be generated by the fundamental flux-density wave of the stator and an extra injected flux-density wave due to current harmonic. Since the excited force-density waves generated in induction machines have a frequency, which is not an integer multiple of the fundamental current frequency in general, a representation of the air-gap flux-density for sub harmonics is required.

Taking the operational slip s of an induction motor into account, the frequency of the additional current does not meet the frequency condition $f = 2\pi f_0 \xi; \quad \xi \in N$, which is required for the Fourier-series-expansion in classic rotating

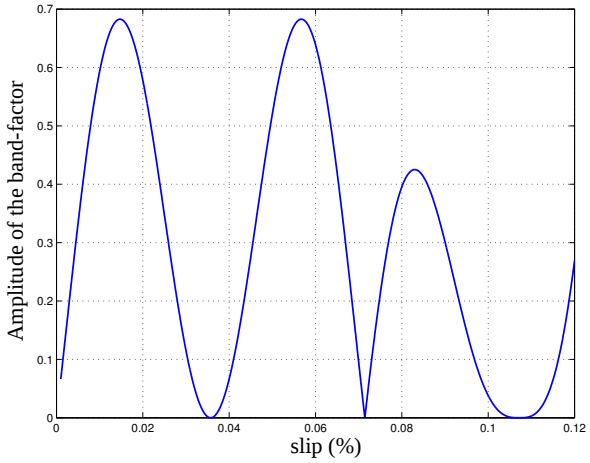

Figure 2. Amplitude of the band-factor for the third rotor harmonic versus the slip ($f_0 = 50$Hz).

field theory [1], [12]. The current can be defined as

$$I = \sum_{\frac{\xi}{m_i}} \hat{I}_{\frac{\xi}{m_i}} \cdot \cos\left(\frac{\xi}{m_i}\left(\omega \cdot t - \frac{k-1}{3} \cdot 2\pi\right)\right). \quad (4)$$

The fundamental frequency of the Fourier-series-expansion f_F is hence chosen to be the greatest common divisor of the stator fundamental f_0 and the slip frequency $f_s = s \cdot f_0$. In this case, the air-gap flux-density field can be expressed by:

$$B(x,t) = \sum_{\xi}\sum_{\nu} 2p \cdot m \cdot q \cdot \frac{\mu_0 N}{2\pi\delta} \cdot k_\omega \cdot \Lambda \cdot A(\nu,\xi) \cdot I \cdot \cos\left(\frac{\xi}{m_i} \cdot (\omega t - \nu x - \varphi)\right); \quad (5)$$
$$\nu = p \cdot g; g \in Z; \xi \in N$$

whereby $2p$ denotes the number of poles, m the number of phases, q the number of slots per pole per phase, N the number of windings per stator coil, δ the air-gap length, k_ω the winding-factor, Λ the permeance-waves, ξ the ordinal number of the injected additional current harmonic. $A(\nu,\xi)$ is a so called band-factor denotes the relationship between the amplitude of a specific current-harmonic and the excited air-gap flux density wave of pole-pair number ν. It is given by:

$$A(\nu,\xi) = \frac{k_\omega}{\nu} \cdot \frac{\sin\left[\pi\left(\frac{\nu}{p} - \frac{\xi}{m_i}\right)\right]}{\sin\left[\pi\left(\frac{\nu}{mp} - \frac{\xi}{mm_i}\right)\right]} \cdot \left(1 + \cos\left[\pi\left(\frac{\nu}{p} - \frac{\xi}{m_i}\right)\right]\right) \quad (6)$$

The term $\frac{\xi}{m_i}$ describes the ordinal number of the current frequency. In contrast to (5) the generated pole pair numbers of the air-gap field are $\nu = p \cdot g$. If the fundamental frequency of the Fourier-series-expansion approaches to the fundamental frequency of the stator phase current, (6) converges to p for $\nu = p\,(6g + \xi)$. Fig. 3 shows the amplitude of the band-factor A versus the frequency order and the pole pair number ν. The higher the absolute value of the band-factor A, the lower is

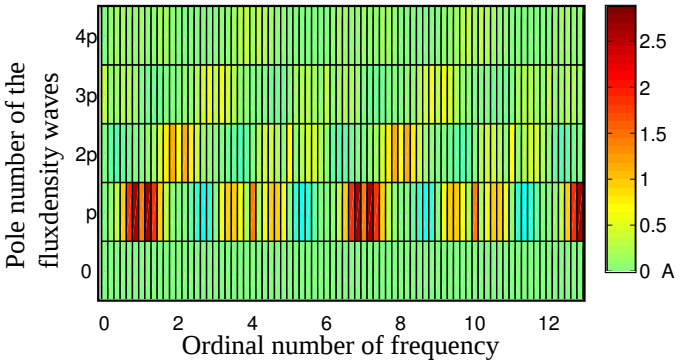

Figure 3. Amplitude of the band-factor A versus the frequency order and the number of poles ($m_i = 6$).

N_1= 36, N_2=28 p=3, s=10% f_1=50Hz		g_1	-4	-3	-2	-1	0	1	2	3	4	
		ν_1	-69	-51	-33	-15	3	21	39	57	75	$f_{\sigma_i, Ord}$
g_2	ν_2		r A	r A	r A	r A	r A	r A	r A	r A	r A	
-3	-81	+ -									-6 0.174	-23.2 -25.2
-2	-53	+ -		-2 0.038						4 0.038		-14.8 -16.8
-1	-25	+ -						-4 0.682				-6.4 -8.4
0	3	+ -					6 0.966 0 0.966					2 0
1	31	+ -			-2 0.682							10.4 8.4
2	59	+ -								2 0.038		18.8 16.8
3	87	+ -										27.2 25.2

Figure 4. Excitation table of the investigated induction motor, whereby ν_1 is the pole-number of the stator field, ν_2 the pole-number of the rotor field, r the mode of the force-density wave and A the amplitude of the band-factor.

the required additional current harmonic for the injection of an additional flux-density wave. In Fig. 3 is shown that flux-density waves with the pole pair numbers p, $2p$ and $3p$ can be generated with discrete frequency orders. They depend on the operational slip s.

III. Determination of Reducible Force-Density Waves

It is possible to generate an additional force-density wave by injection of only one flux-density wave with sufficient amplitude according to equation (3). In order to keep parasitic effects, due to air-gap flux-density harmonics of the additional current, as small as possible, the fundamental flux-density wave of the motor is chosen to be one of the convolutions. Oppose to claimed in [9], force-density countershafts with circumferential modes $r = 0$, $\pm 2p$, $\pm 3p$ and $\pm 4p$ can be generated with reasonably low amplitudes of the current harmonics, which can be seen from the computation of the band factor in Fig. 3. However, the reducibility of a force-density wave is constrained by the operational slip. Fig. 2 shows the intense sensitivity of the band-factor, in this case for the third rotor harmonic, versus the slip. The amplitudes of the band-factor for different force-density waves for an exemplary operation point is given in Fig. 4.

The frequency, pole pair number and phase angle of the additional required flux-density wave can be calculated according

to equation-set (3) from the properties of the countershaft:

$$\begin{aligned} f_+ &= f_{\text{counter}} \mp f_{\text{fund}} \\ \nu_+ &= \nu_{\text{counter}} \mp \nu_{\text{fund}} \\ \varphi_+ &= \varphi_{\text{counter}} \mp \varphi_{\text{fund}} \end{aligned} \tag{7}$$

whereby the index $_+$ describes the additional flux-density wave injected by a current harmonic, the index $_{\text{fund}}$ describes the fundamental flux-density wave and the index $_{\text{counter}}$ the countershaft. The phase of the countershaft complies to the phase of the found force-density wave, but is shifted by π.

The relation between the phase angle of a flux-density wave and its generating current depends on the frequency. Since there are two currents with different frequencies, the fundamental and the additional one, two FE simulations are applied in order to approximate the phase angle of the additional current harmonic. One simulation is performed without current injection and one simulation only taking into account the extra current. The phase angle of the additional current is subsequently approximated according to equation (8) in case of addition and (9) in case of subtraction in convolution (3),

$$\varphi_{\text{i+}} = \varphi_{\text{counter}} - \varphi_{\text{fund}} - \varphi_{\text{b+}} + 2 \cdot \varphi_{\text{i}_{\text{fund}}} \tag{8}$$

$$\varphi_{\text{i+}} = \varphi_{\text{counter}} + \varphi_{\text{fund}} - \varphi_{\text{b+}} \tag{9}$$

whereby $\varphi_{\text{i+}}$ denotes the phase angle of the additional current and $\varphi_{\text{b+}}$ the phase angle of the additional flux-density wave to its generating current. In case of summation $\varphi_{\text{i}_{\text{fund}}}$ has to be considered, which is the phase angle of the fundamental current.

Fig. 5 illustrates the phase angle relations for the case of summation. The phase angle $\varphi_{\text{i}_{\text{fund}}}$ is selected to be zero.

In order to evaluate the proposed approach FE simulations of a standard industrial induction motor with $N_1 = 36$ stator slots, $N_2 = 28$ rotor slots, 6 poles are performed. For this example a fundamental frequency of 50Hz and a slip of 10% is selected. The rated power of the investigated machine is $P = 800$W. The band-factor A has the maximum for pole pair number p, in this case $p = 3$, Fig. 3. A force-density wave with the circumferential order $r = p_{\text{counter}} - p_{\text{fund}} = 3-3 = 0$ and frequency order 108 is selected. The spectrum of the force-density waves with circumferential mode 0 without countershaft is presented in Fig. 6. The amplitude of the band-factor, see (6), for this operating point and force-density wave results in $A = 0.682$, which will fulfill the requirement of a small additional current. The pole number, frequency and phase shift of the injected flux-density wave are calculated according to equations (7) and (9). The amplitude of the extra current is calculated by:

$$\hat{I}_+ = \frac{\hat{\sigma}_{\text{counter}} 2\mu_0}{2p \cdot m \cdot q \cdot \frac{\mu_0 N}{2\pi\delta} \cdot k_\omega \cdot \Lambda \cdot A \cdot \hat{B}_{\text{fund}}} \cdot k_\omega \tag{10}$$

It is found, that the phase angle of the injected force-density wave is strongly dependent on the non-linear magnetic material properties and the interaction of the injected flux-density waves with the existent air-gap harmonics, thus the force-density wave is only slightly reduced if the analytically determined current I_+ and phase is used from (9) and (10), receptively. . Therefore, an FE simulation set is used for the

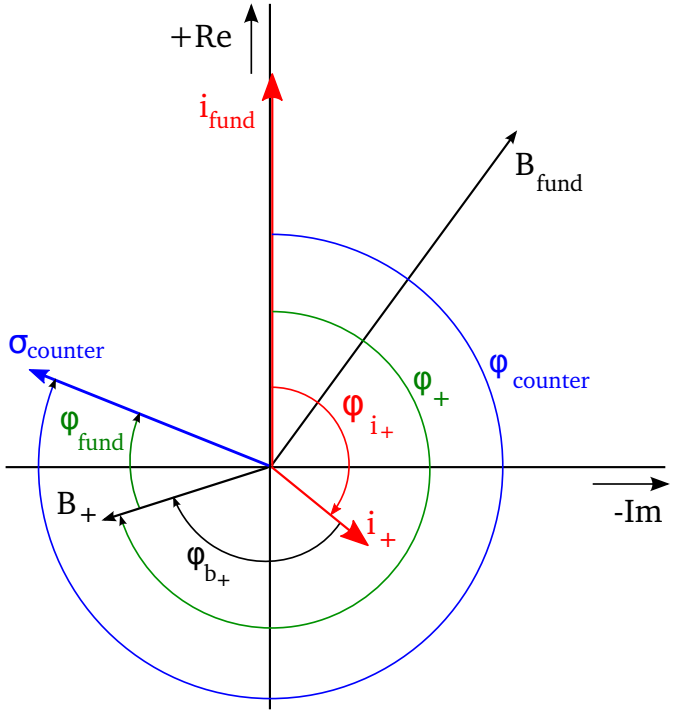

Figure 5. Phase angle relations in case of additional flux-density waves, ($\phi_{i_{fund}} = 0$).

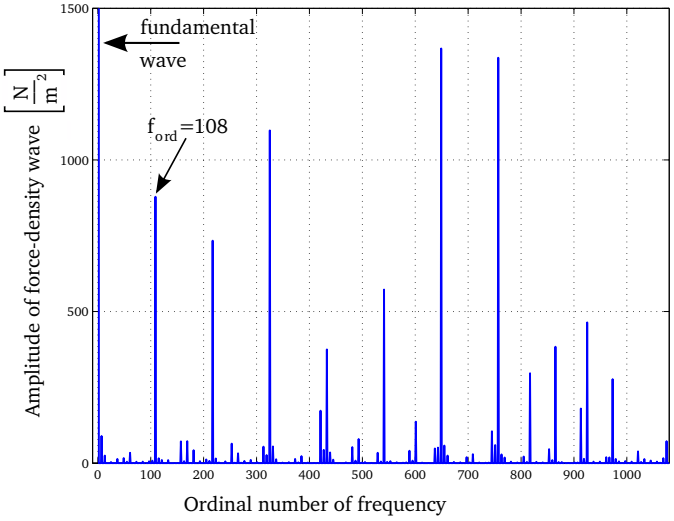

Figure 6. Force-density waves with $r = 0$, with sinusoidal current.

determination of an optimal phase angle. Starting with the pre-calculated phase angle based on equation (9) a parameter variation is performed. It is found, that the parameter phase angle of the additionally imposed current is robust, i.e. small errors in the pre-calculated phase angle do not lead to higher radial force-density waves. Based on the presented approach the amplitude $\hat{I}_+$, the frequency f_+ and the phase angle φ_+ is calculated. These calculated properties are shown in Tab. I. Therewith, an FE simulation of the radial force-density waves is performed to verify the results. The spectrum of the force-density waves with circumferential mode 0 with this countershaft is presented in Fig. 7. With the optimised values, the studied force-density wave is reduced from $818\frac{N}{m^2}$

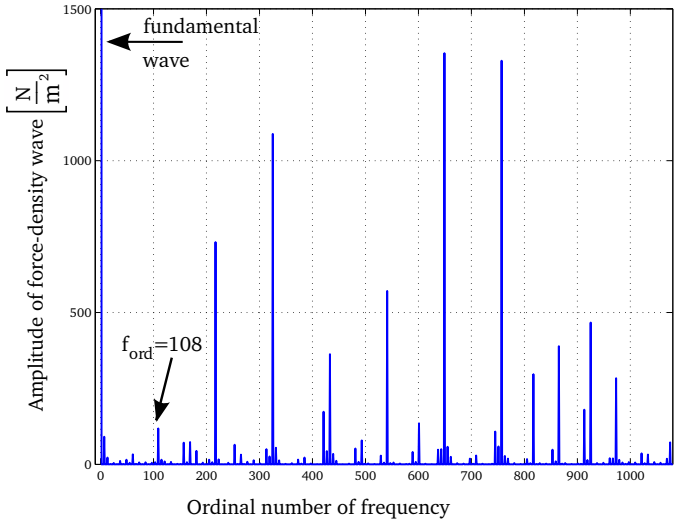

Figure 7. Force-density waves with $p = 0$, with optimized additional current harmonic.

Table I
FUNDAMENTAL CURRENT, OPTIMIZED ADDITIONAL CURRENT AND IMPACT ON THE FORCE-DENSITY WAVE.

I_0	φ_0	I_+	φ_+	σ_{before}	σ_{red}
$2A$	$0°$	$0.044A$	$-213°$	$878\frac{\text{N}}{\text{m}^2}$	$118\frac{\text{N}}{\text{m}^2}$

to $118\frac{N}{m^2}$.

IV. PARASITIC EFFECTS BY THE ADDITIONAL CURRENT HARMONICS

Two kinds of parasitic effects are studied in the presented research. The first one is the increase of radial force-density waves, which have not been regarded in the reduction procedure. The second one is the influence on torque pulsation. In case of the radial force-density waves the strongest interaction is expected with the sum of the fundamental and additional flux-density wave in the convolution of equation (3), i.e. circumferential mode $r = -2p = -6$ and ordinal frequency number 168. In the reviewed example the previously existent force-density wave of the circumferential mode $r = -2p = -6$ and ordinal frequency number 168 is reduced as well from $614\frac{N}{m^2}$ to $52\frac{N}{m^2}$. In case of the studied induction motor the highest amplitudes of force-density waves are expected with mode numbers $|r| = 0$ and $|r| = 6$. The parasitic effect on these waves is studied in more detail. In order to evaluate the influence on force-density waves with these two mode numbers the difference of the amplitudes of the force-density waves $\hat{\sigma}_{r,i}$ (whereby r is the mode and i is the frequency order of the force-density wave) with and without optimized current shape is analyzed. In Fig. 8 and Fig. 9 the difference of the force-density waves $\Delta = \hat{\sigma}_{\text{fund},r,i} - \hat{\sigma}_{\text{counter,r,i}}$ of the fundamental simulation without countershaft and the simulation with countershaft for the mode numbers $r = 0$ and $r = -6$ respectively is shown. It is verified that only the intended force-density waves are reduced, and the influence on the other frequencies is low as well. The influence of the additional current harmonic on force-density waves with other circumferential modes is observed to be low. The evaluation of

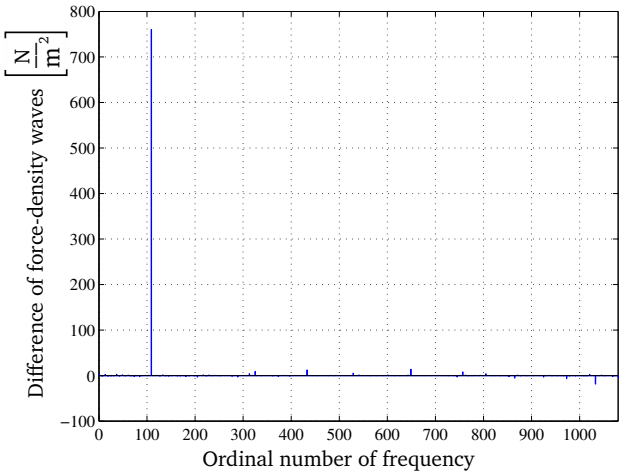

Figure 8. Difference of force-density waves with $r = 0$, without and with optimised additional current harmonic.

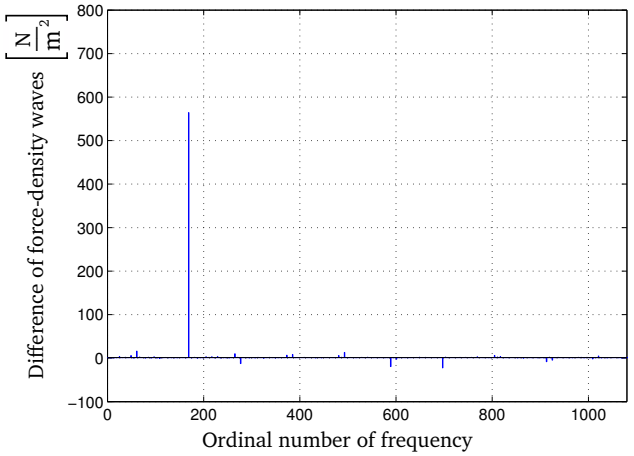

Figure 9. Difference of force-density waves with $r = -6$, without and with optimised additional current harmonic.

the parasitic effects on the torque is performed by means of a Fourier-analysis of the torque for one revolution of the rotor. Two FE simulations are compared, the one with sinusoidal current and the one with the optimized current shape. Fig. 10 and Fig. 11 show the spectrum of the torque for both simulations. As shown, the influence of the extra current on the torque is low. The constant component of the torque is $T_0 = 4.26$ Nm. No change in this component is determined. The first relevant harmonic of the torque is increased from $T_1 = 0.62$ Nm to $T_1 = 0.64$ Nm. This increase is can be considered negligible to be negligible. Therefore, the method is evaluated to be interesting for further research. The influence of the additional current on the efficiency of the motor is expected to be low, since the amplitude of the fundamental current is $\hat{I}_0 = 2$ A and the amplitude of the extra current is $\hat{I}_+ = 0.044$ A (i.e. 2.2% of the rated stator current). An increase of the stator and rotor copper and iron losses is expected.

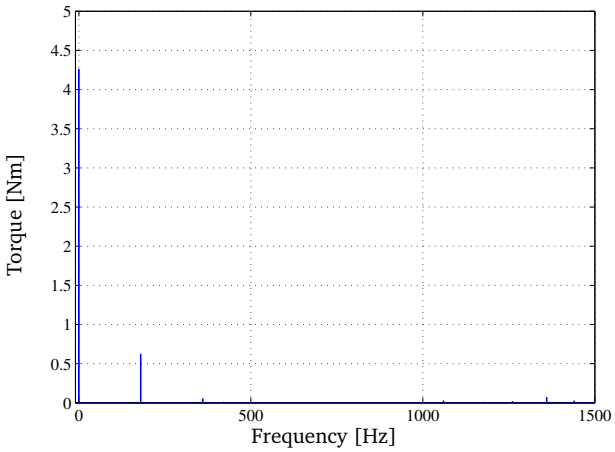

Figure 10. Fourier transform of the torque, sinusoidal current.

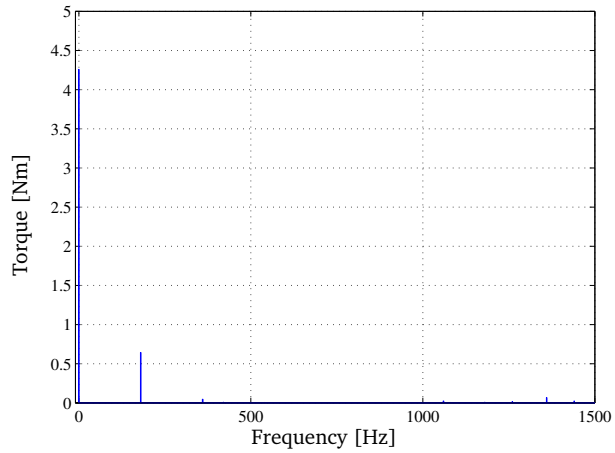

Figure 11. Fourier transform of the torque, with optimised additional current harmonic.

V. Conclusions

This paper presents an approach to reduce radial force-density waves with harmonic current injection of low-power. In contrast to [9], [10], [14] analytic formulas for the pre-calculation of the amplitude, frequency and phase angle of the additional current are presented. It is found that the force-density waves with the circumferential mode $r = 0$, $\pm 2p$, $\pm 3p$ and $\pm 4p$ can be reduced with reasonably low current amplitude. Oppose to [9], it is found that the frequency of the reducible force-density wave depends on the slip. The proposed approach is evaluated and verified by means of FE simulations. The results of the numeric simulation are in good agreement with the analytical pre-calculated properties of the additional current harmonic for the reduction of a particular force-density wave. However, a further reduction of the aimed force-density wave after applying an FE simulation set is accomplished. The study reveals that the exact knowledge of the phase angle is not required; the presented approach shows robustness concerning the accuracy of the pre-calculated phase angle. Parasitic effects of the additional current harmonic towards other radial force-density waves and torque pulsation is studied. It is found that the influence on parasitic force-density waves is low for the studied case. Since the amplitude of the additional current harmonic is only 2.2% of the fundamental current, no significant effect on the torque spectrum is determined.

This approach seems promising to the authors, therefore further research is planned. A test bench for the experimental validation is scheduled. In the first step a variable non-switching source will be applied. Further steps are voltage driven simulations, the investigation of manufacturing tolerances, the influence of standard *PWM* inverters and adaptive determination of the additional current harmonic properties (amplitude and phase) by means of measurements.

References

[1] H. Jordan, *Geräuscharme Elektromotoren*. Girardet, 1950.
[2] L. Timar, P, A. Fazekas, J. Kiss, A. Miklos, and G. Yang, S, *Noise and Vibration of Electrical Machines*. Elsevier, 1989.
[3] T. Habetler and D. Divan, "Acoustic noise reduction in sinusoidal pwm drives using a randomly modulated carrier," in *20th Annual IEEE Power Electronics Specialists Conference, PESC '89*, June 1989, pp. 665–671.
[4] J. Boys and P. Handley, "Spread spectrum switching: low noise modulation technique for pwm inverter drives," *Electric Power Applications, IEE Proceedings B*, vol. 139, no. 3, pp. 252 –260, may. 1992.
[5] G. Covic and J. Boys, "Noise quieting with random pwm ac drives," *Electric Power Applications, IEE Proceedings* -, vol. 145, no. 1, pp. 1 –10, jan. 1998.
[6] J. Gieras, C. Wang, and J. C. Lai, *Noise of polyphase electric motors*. CRC Press Taylor&Francis Group, 2006.
[7] A. Ruiz-Gonzalez, M. Meco-Gutierrez, F. Perez-Hidalgo, F. Vargas-Merino, and J. Heredia-Larrubia, "Reducing acoustic noise radiated by inverter-fed induction motors controlled by a new pwm strategy," *IEEE Transactions on Industrial Electronics*, vol. 57, no. 1, pp. 228 –236, Jan. 2010.
[8] S. Garcia-Otero and M. Devaney, "Minimization of acoustic noise in variable speed induction motors using a modified pwm drive," *Industry Applications, IEEE Transactions on*, vol. 30, no. 1, pp. 111–115, Jan/Feb 1994.
[9] B. Cassoret, R. Corton, D. Roger, and J.-F. Brudny, "Magnetic noise reduction of induction machines," *IEEE Transactions on Power Electronics*, vol. 18, no. 2, pp. 570–579, 2003.
[10] D. Belkhayat, D. Roger, and J. Brudny, "Active reduction of magnetic noise in asynchronous machine controlled by stator current harmonics," in *Eighth International Conference on Electrical Machines and Drives, 1997 (Conf. Publ. No. 444)*, 1997, pp. 400–405.
[11] R. Corton, B. Cassoret, and J. Brudny, "Characterisation of three-phase harmonic systems generated by pwm inverter switching application to induction machine magnetic noise reduction," in *Electric Machines and Drives Conference, 2001. IEMDC 2001. IEEE International*, 2001, pp. 442 –447.
[12] K. Oberretl, "Losses, torques and magnetic noise in induction motors with static converter supply, taking multiple armature reaction and slot openings into account," *Electric Power Applications, IET*, vol. 1, no. 4, pp. 517–531, 2007.
[13] C. Wang and J. C. S. Lai, "Vibration analysis of an induction motor," *Journal of Sound and Vibration*, vol. 224, pp. 733–756, 1999.
[14] I. Karkkainen and A. Arkkio, "Harmonic torque suppression by manual voltage injection," in *Electrical Machines (ICEM), 2010 XIX International Conference on*, 2010, pp. 1 –6.
[15] Z. Zhu, Y. Liu, and D. Howe, "Minimizing the influence of cogging torque on vibration of pm brushless machines by direct torque control," *Magnetics, IEEE Transactions on, Magnetics, IEEE Transactions on*, vol. 42, no. 10, pp. 3512–3514, 2006.
[16] M. Hafner, D. Franck, and K. Hameyer, "Static electromagnetic field computation by conformal mapping in permanent magnet synchronous machines," *Magnetics, IEEE Transactions on*, vol. 46, no. 8, pp. 3105 –3108, 2010.
[17] D. Zarko, "A systematic approach to optimized design of permanent magnet motors with reduced torque pulsations," Ph.D. dissertation, University of Wisconsin, Madison, Jul. 2004.
[18] M. van der Giet, R. Rothe, and K. Hameyer, "Asymptotic Fourier decomposition of tooth forces in terms of convolved air gap field harmonics for noise diagnosis of electrical machines," *COMPEL*, vol. 28, no. 4, pp. 804–818, 2009.